

The carbon dioxide evasion cycle of an intermittent first-order stream: contrasting water–air and soil–air exchange

Arún Looman · Damien T. Maher · Elise Pendall · Adrian Bass · Isaac R. Santos

Received: 7 July 2016 / Accepted: 22 December 2016 / Published online: 30 December 2016
© Springer International Publishing Switzerland 2016

Abstract Ephemeral streams and wetlands are characterized by complex cycles of submersion and emersion, which influence the greenhouse gas flux rates. In this study we quantify the spatiotemporal variability in CO₂ and CH₄ concentrations and fluxes of an intermittent first-order stream over three consecutive wet and dry cycles spanning 56 days, to assess how hydrologic phase transitions influence greenhouse gas evasion. Water column excess CO₂ ranged from –11 to 1600 μM, and excess CH₄ from 1 to 15 μM. After accounting for temporal changes in

the ratio of wet versus dry streambed hydraulic radius, total CO₂–C fluxes ranged from 12 to 156 mmol m⁻² day⁻¹, with an integrated daily mean of 61 ± 25 mmol m⁻² day⁻¹. Soil–air evasion rates were approximately equal to those of water–air evasion. Rainfall increased background water–air CO₂–C fluxes by up to 780% due to an increase in gas transfer velocity in the otherwise still waters. CH₄–C fluxes increased 19-fold over the duration of the initial, longer wet-cycle from 0.1 to 1.9 mmol m⁻² day⁻¹. Temporal shifts in water depth and site-specific ephemerality were key drivers of carbon dynamics in the upper Jamison Creek watercourse. Based on these findings, we hypothesise that the cyclic periodicity of fluxes of biogenic gases from frequently intermittent streams (wet and dry cycles ranging from days to weeks) and seasonally ephemeral watercourses (dry for months at a time) are likely to differ, and therefore these differences should be considered when integrating transient systems into regional carbon budgets and models of global change.

Responsible Editor: Jennifer Leah Tank.

Electronic supplementary material The online version of this article (doi:10.1007/s10533-016-0289-2) contains supplementary material, which is available to authorized users.

A. Looman (✉) · D. T. Maher · I. R. Santos
National Marine Science Centre, Southern Cross
University, Coffs Harbour, NSW, Australia
e-mail: arun.looman@hotmail.com

A. Looman · D. T. Maher · I. R. Santos
School of Environment, Science, and Engineering,
Southern Cross University, Lismore, NSW, Australia

E. Pendall · A. Bass
Hawkesbury Institute for the Environment, Western
Sydney University, Richmond, NSW, Australia

A. Bass
Department of Geographical and Earth Sciences,
University of Glasgow, Glasgow, UK

Keywords Ephemeral · Greenhouse gas · Methane · Headwater stream · Air–water flux

Introduction

The exchange of carbon dioxide (CO₂) and methane (CH₄) between inland waters and the

atmosphere is a dynamic process. Variability in the fluxes of CO₂ and CH₄ at the water- and soil-to-air interfaces is influenced by multiple factors including seasonality (Rudorff et al. 2011; Peter et al. 2014), atmospheric forcing (e.g. rainfall, wind velocity; Frew et al. 2004; Ho et al. 2007; Dinsmore and Billett 2008), stream hydraulics (Alin et al. 2011; Raymond et al. 2012), groundwater discharge (Jones and Mulholland 1998; Sadat-Noori et al. 2015), and metabolism (Tamooh et al. 2013). In flowing waters, the partial pressure of CO₂ (*p*CO₂) can vary over orders of magnitude both spatially (Koprivnjak, et al. 2010; Weyhenmeyer et al. 2012; Teodoru et al. 2015), and temporally (Johnson et al. 2007; Bass et al. 2014; Ruiz-Halpern et al. 2015; Looman et al. 2016; Tweed et al. 2016). This variability, along with a limited extent of available data and the lack of a modelling framework for many aquatic systems (Raymond et al. 2013; Regnier et al. 2013), complicates the quantification of greenhouse gas (GHG) emissions from inland waters as well as our understanding of their role in the global carbon (C) cycle (Battin et al. 2009). Seasonally ephemeral and frequently intermittent low order streams are extensive components of the fluvial network, and to date there is limited understanding on the spatial and temporal variability of water- and soil-to-air GHG exchange rates in these systems (von Schiller et al. 2014).

Temporary watercourses can comprise more than 50% of the total drainage network length within water catchments (Hansen 2001; Nadeau and Rains 2007), and are particularly common to headwaters (Costigan et al. 2015). The extent of perennial versus non-perennial segment length in these systems is, however, not constant, due to a cyclic continuum of network extension, contraction and fragmentation (von Schiller et al. 2015). In landscapes where discontinuity of flow is particularly pronounced even Strahler order delineations (Strahler 1957) can be dynamic, shifting by up to two orders between seasonal extremes (Datry et al. 2014; Godsey and Kirchner 2014). For unregulated rivers, Haines et al. (1988) described 15 seasonally-based flow regime classes, of which three describe the natural zero-flow sequences commonly found in Australia (McMahon and Finlayson 2003): (1) perennial streams with high annual variability that cease to flow in extreme years; (2) ephemeral streams that regularly

cease to flow in the dry season; and (3) arid zone streams with long and erratic periods of no flow.

In non-perennial watercourses the frequency and duration of natural hydrologic fragmentation relates to site-specific attributes such as annual precipitation, ambient temperature, riparian vegetation-streamflow interactions, watercourse shade dynamics, topography, slope, geomorphology, groundwater levels and sedimentology (Leopold and Maddock 1953; Shaw and Cooper 2008; Salemi et al. 2012; Snelder et al. 2013). In anthropogenically-modified environments, the wet and dry cycle recurrence interval can be further influenced by factors such as urbanisation (impermeable surfaces), the presence/absence of serial discontinuities (e.g. weirs, impoundments), and groundwater or surface water abstraction (Holmes 1999; Stanford and Ward 2001; Steward et al. 2012). McMahon and Finlayson (2003) use the term “anti-drought” to describe the regulated addition of larger or more persistent flows to the natural hydrologic regime during dry or low-flow intervals, resulting in artificial wet and dry cycle intermittence.

Hydrologic phase transitions such as that from baseflow to stormflow can give rise to hot spot and hot moment phenomena of accelerated rates in the spiralling of dissolved carbon and nutrients in perennial inland waters (McClain et al. 2003; Hook and Yeakley 2005; Raymond and Saiers 2010; Janke et al. 2014; Raymond et al. 2016). In ephemeral watercourses, other transitions such as streambed drying and rewetting can alter the rates of macromolecular decomposition (Dieter et al. 2011), biofilm metabolism and community structure (Timonser et al. 2012; Fazi et al. 2013; Sabater et al. 2016), as well as connectivity between adjacent pools (Larned et al. 2010; Bernal et al. 2012; Casas-Ruiz et al. 2016). The coupled influence of such transition processes on the rate of GHG fluxes from ephemeral waters, however, remains largely unknown. In the present study, we quantify the spatial flux as well as temporal changes to the CO₂ and CH₄ dynamics of an intermittent first-order stream (Jamison Creek, Blue Mountains, Australia) over three consecutive wet and dry cycles occurring over a 56-day period. Our primary objectives were: (1) to quantify variability in CO₂ emissions from wet versus dry portions of the stream reach during episodes of expansion and contraction; (2) to assess changes in CO₂ and CH₄ fluxes within the study segment over time; and, (3) to evaluate the significance of rain events on GHG emissions.

Methods

Study site

Field investigations were performed in the headwaters of the upper Jamison Creek watercourse in the Greater Blue Mountains World Heritage Area of New South Wales, Australia (33°42'S, 150°22'E; 867 mASL; Fig. 1), west of the Sydney Basin. The mean annual ambient temperature at the nearest meteorological station in Katoomba is 12.4 ± 4.4 °C and mean annual precipitation 1405 ± 35 mm (1885–2016 period; Station #063039; BoM 2015a). There are on average 162 days influenced by rainfall annually, with mean rainfall rates of ≥ 1 , ≥ 10 and ≥ 25 mm day⁻¹ for 108, 39 and 15 days, respectively.

The catchment sediments are derived from Hawkesbury and Narrabeen Group sandstones and are predominantly siliceous, with localised peat deposits and claystone interbeds (Fryirs et al. 2016). Streambed sediments are of sandy-loam textural class, with occasional Fe mottles indicative of changeable hyporheic zone redox chemistry. In-stream flora was dominated by *Cyperus eragrostis* and *Rumex obtusifolius*. Vegetative coverage of the less-frequently inundated upstream study segments (sites S1 and S2, see below for details) varied from ~20% in winter to ~50% by the end of the sampling period in mid-

spring. The more-frequently inundated downstream study segments were, in contrast, void of in-stream vegetation. During the wet cycles, biofilms and filamentous chlorophytes were also present.

Experimental approach

Measurements were taken from the uppermost 100 m of the watercourse, which has been modified (e.g. straightened) to connect a 36 ha golf course to Lake Wentworth, a flooded Temperate Highland Peat Swamp on Sandstone (an endangered ecological community; TSSC 2005). The study segment was further reduced to five shorter sub-reaches spanning 5.7–20.1 m in length (sites S1–S5; Fig. 1) according to conditions of observed disconnection during periods of low stage height. For time series observations, all data were collected at the upstream S1 site over a 56-day time period during the winter-spring transition (23 August–17 October, 2015; modified channel), and, for spatial observations, all sites were surveyed during two separate wet-cycles when the stream was disconnected (11/9 and 21/09; Table 1). Study segment S2 was located inside a roadway culvert and sites S3–S5 represented a channelised, non-flooded section of the peat swamp.

We sampled pH, conductivity, temperature, and dissolved oxygen (DO) concentrations in situ with a



Fig. 1 Map of the upper Jamison Creek watercourse and study sites S1–S5. Source ArcGIS 10.3. (ESRI; Redlands, CA)

Table 1 Mean between-site variability in water quality parameters (\pm SD), apparent oxygen utilisation (AOU), excess CO_2 , excess CH_4 , mean water–air flux rates (F) for CO_2 and CH_4 , and water column morphology for study sites S1–S5 during the 2 days of spatial sampling

Site	Water temp. ($^{\circ}\text{C}$)	pH	Sp. Cond. ($\mu\text{s cm}^{-1}$)	AOU (μM)	Excess CO_2 (μM)	Excess CH_4 (μM)	F- CO_2 ($\text{mmol C m}^{-2} \text{ day}^{-1}$)	F- CH_4 ($\text{mmol C m}^{-2} \text{ day}^{-1}$)	Wetted length (m)	Wetted width (m)	Stage height (m)
S1	14.5 \pm 4.7	5.87 \pm 0.31	89 \pm 6	93 \pm 91	733 \pm 495	12.9 \pm 2.4	36.0 \pm 24.3	1.7 \pm 0.3	14.4	1.0	0.1
S2	10.2 \pm 0.6	6.05 \pm 0.43	101 \pm 6	265 \pm 56	531 \pm 389	2.6 \pm 0.9	26.1 \pm 19.1	0.3 \pm 0.1	2.4	2.1	0.2
S3	13.2 \pm 1.0	5.52 \pm 0.48	72 \pm 3	155 \pm 0	1390 \pm 227	0.4 \pm 0.0	68.3 \pm 11.2	0.1 \pm 0.0	16.2	0.5	0.3
S4	14.9 \pm 0.4	5.63 \pm 0.32	70 \pm 3	114 \pm 1	760 \pm 61	6.4 \pm 2.8	37.4 \pm 3.0	0.9 \pm 0.4	8.4	1.6	0.4
S5	15.0 \pm 0.5	5.89 \pm 0.40	61 \pm 2	120 \pm 23	326 \pm 32	4.3 \pm 0.7	16.0 \pm 1.6	0.6 \pm 0.1	5.7	1.2	0.4

Hydrolab DS5X multiparameter sonde. pH and conductivity were calibrated against pH_{NBS} buffers 4.00 and 7.00 and conductivity against a $1410 \mu\text{S cm}^{-1}$ solution. The sonde was recalibrated at the start and end of each rewetting cycle. Ambient temperature, wind speed, rainfall rate and barometric pressure were measured with a portable weather station fitted with a cup anemometer (Davis Instruments, USA), located central to the Jamison Creek catchment 1.2 km from the study site. Evapotranspiration data was obtained from the Mount Boyce meteorological station ($33^{\circ}36'\text{S}$, $150^{\circ}16'\text{E}$; Station #063292; BoM 2015b), 14.5 km away.

To account for temporal changes in the ratio of wet versus dry surface area, we measured stream depth and width at $30 \times 30 \text{ cm}$ intervals under conditions of high stage (i.e. using the water level as a reference datum) to create a detailed bathymetric digital elevation model (DEM) of the study segment. Relative change in stage height (positive or negative) was recorded at a fixed datum in sub-reach S1, and, using this datum, we then determined the subsequent mean wetted channel width (w , m), mean water depth (d , m), water volume (V , m^3), and water-to-soil ratios for each sampling interval. To estimate streamwater velocity, we formulated a discharge-rating curve from the continuity relationship $Q = dwv$ and interpolated v from gauge heights above $Q = 0$ via cubic polynomial function (Xia et al. 2010), where Q is the discharge in $\text{m}^3 \text{ s}^{-1}$ and v is velocity in m s^{-1} .

Dissolved gas analyses

Streamwater $p\text{CO}_2$ and $p\text{CH}_4$ were sampled 1–7 times daily from half the depth of the water column using a syringe headspace method (Borges et al. 2015) whereby four replicate syringes (Terumo, Japan), each fitted with a three-way stopcock, were used to equilibrate 30 ml of bubble-free sample water with 30 ml of N_2 gas. To reduce permeability to gas, each syringe was periodically coated with a thin film of petroleum jelly (Vaseline, Unilever). Replicate samples were equilibrated by shaking for 5–10 min and end-temperature measured with a mercury thermometer. The partial pressure of CO_2 in the equilibrated headspace gas was measured using an IRGA (LiCor LI-820), then converted to the fugacity of CO_2 ($f\text{CO}_2$) using:

$$f\text{CO}_2 = p\text{CO}_2 \cdot f(g) \quad (1)$$

where $f(g)$ is the fugacity coefficient (unitless; Millero 2007). The optical path of the IRGA was kept dry between measurements using a desiccant (Drierite). We then calculated $[\text{CO}_2^*]$ {i.e. the sum of $[\text{CO}_2]$ and $[\text{H}_2\text{CO}_3]$ } according to Henry's Law:

$$[\text{CO}_2^*] = K_{0,\text{CO}_2} \cdot f\text{CO}_2 \quad (2)$$

where K_{0,CO_2} is the CO_2 solubility constant at given temperature and salinity in $\text{mol L}^{-1} \text{atm}^{-1}$ (Weiss 1974). The IRGA was calibrated using five gas standards ranging from zero to 18,100 ppm CO_2 in nitrogen ($\pm 2\%$). To correct for spatial and temporal thermal variability, CO_2 partial pressures reported herein were normalised to the mean daily water temperature of 11.8 °C. CH_4 was also sampled using the above-described syringe headspace method, whereby 240 ml of headspace gas from eight co-equilibrated syringes was transferred to an evacuated 0.5 L Tedlar bag (Restek, USA) and stored at 5 to 10 °C for transportation to the lab where analyses were performed on a calibrated Cavity Ring-down Spectrometer (G2201-*i*, Picarro, USA) within 2-h of sampling. To account for diel variability in O_2 and CO_2^* concentrations, samples were collected at least two times per day for 50% of sampling days and included morning and evening sampling. Additional sampling was conducted to characterise natural diel fluctuations at the S1 site during conditions of disconnect, as well as shorter-term variability induced by rainfall. Where only one sample was collected per day samples were preferentially collected late morning to approximate the diel mean (Supplementary Table A2).

We present dissolved gas concentrations as excess CO_2 , excess CH_4 and apparent oxygen utilization (AOU), being the deviation of each of these gases from atmospheric equilibrium (x_{eq} ; where x is the dissolved gas of interest; Richey et al. 1988):

$$\text{Excess CO}_2 = [\text{CO}_2^*] - [\text{CO}_2\text{eq}] \quad (3)$$

$$\text{Excess CH}_4 = [\text{CH}_4] - [\text{CH}_4\text{eq}] \quad (4)$$

$$\text{AOU} = [\text{O}_2\text{eq}] - [\text{O}_2] \quad (5)$$

where $[\text{O}_2]\text{eq}$ was calculated from dissolved oxygen % saturation measurements and $[\text{CO}_2]\text{eq}$ and $[\text{CH}_4]\text{eq}$ were calculated from atmospheric samples collected in situ, using barometric pressure, temperature and salinity.

Chamber deployments and modelling

Water–air CO_2 fluxes were measured in duplicate on 10 occasions using a lightweight static free-floating chamber (diameter, 300 mm; height, 140 mm; water column penetration, 30 mm), integrated into a recirculating closed loop with the IRGA using a microdiaphragm air pump (Parker, USA) and an inline desiccant (Drierite). Soil-to-air CO_2 fluxes from the dry streambed were measured in duplicate on 11 occasions using a second chamber (diameter, 150 mm; height, 100 mm), which was lowered onto a fixed collar using the same closed-loop system. Chamber fluxes (F , $\text{mmol m}^{-2} \text{day}^{-1}$) were calculated from the rate of change in chamber $p\text{CO}_2$ over time (Frankignoulle 1998):

$$F_{\text{CO}_2} = \left(\frac{d(p\text{CO}_2)}{dt} \right) \left(\frac{V}{RT_K S} \right) \quad (6)$$

where $d(p\text{CO}_2)/dt$ is the slope of the CO_2 accumulation inside the chamber ($\mu\text{atm s}^{-1}$), V is the chamber volume (L), T_K is ambient atmospheric temperature in degrees kelvin (K), S is the chamber surface area (m^2), and R is the universal gas constant ($\text{L atm K}^{-1} \text{mol}^{-1}$). Deployment durations were typically <5 min and observed increase of $p\text{CO}_2$ inside the chamber was linear for 97% of chamber measurements ($r^2 \geq 0.95$).

For background fluxes, we derived gas transfer velocities (k , in m day^{-1}) at the boundary layer interface from our floating chamber measurements, and converted $k\text{-CO}_2$ to $k\text{-CH}_4$ using temperature-dependent Schmidt numbers (Sc_T) suitable for freshwater (Jähne et al. 1987; Wanninkhof 2014):

$$k_{600} = k_{\text{CO}_2} / (Sc_T/600)^{-n} \quad (7)$$

$$k_{\text{CO}_2} / k_{\text{CH}_4} = (Sc_{\text{CO}_2} / Sc_{\text{CH}_4})^{-n} \quad (8)$$

where n is the Schmidt number exponent depending on the condition of the aquatic boundary layer, which was set at 0.67 for lentic waters or 0.5 for flowing waters applying an arbitrary cut off value of a mean daily v of 0.1 m s^{-1} . We used the measured $k\text{-CO}_2$ and calculated $k\text{-CH}_4$ to estimate the flux for each gas according to:

$$F_{\text{CO}_2} = k_{\text{CO}_2} \cdot K_{0,\text{CO}_2} (f\text{CO}_{2,\text{water}} - f\text{CO}_{2,\text{air}}) \quad (9)$$

$$F_{\text{CH}_4} = k_{\text{CH}_4} \cdot K_{0,\text{CH}_4} (p\text{CH}_{4,\text{water}} - p\text{CH}_{4,\text{air}}) \quad (10)$$

where $\text{CO}_{2,\text{water}}/\text{CH}_{4,\text{water}}$ and $\text{CO}_{2,\text{air}}/\text{CH}_{4,\text{air}}$ are the fugacity (f) or partial pressures (p) of each gas in the surface water and overlying atmosphere, respectively (Bakker et al. 2014), and K_{0,CH_4} is the CH_4 solubility according to the coefficients of Yamamoto et al. (1976).

Direct water–air flux measurements using floating chambers were excluded during hydrologic phase transitions as this method does not account for the influence of physical forcing by rainfall on the aquatic boundary layer and because anchored chambers tend to over-estimate fluxes in turbulent waters (Lorke et al. 2015). Thus, to account for the influence of rewetting events on k we also modelled our data empirically using two approaches, “HO” and “RAY”, based on rainfall rate, Ho et al. (1997) and event-induced water velocity, Raymond et al. (2012), respectively:

$$k_{600}(\text{HO}) = 0.929 + 0.679R_n - 0.0015R_n^2 \quad (11)$$

$$k_{600}(\text{RAY}) = (vs)^{0.89} \cdot d^{0.54} \cdot 5037 \quad (12)$$

where R_n is the rain rate (mm h^{-1}), v is the water velocity (m s^{-1}), s is the slope of the study segment (unitless), and d is water depth (m).

Statistical analyses and hydrologic delineations

For statistical analyses of C-gas species with environmental and morphological variables we used Pearson's least square regression for linear covariance (StatPlus, AnalystSoft Inc.), with significance herein implied at the 95% confidence interval ($p < 0.05$). Wet and dry cycles at the S1 study site were delineated using a water-to-soil ratio of 0.5, which coincided with a daily mean stage height of 0.0 m.

Results

Stream morphometry and ancillary variables

Throughout the 56-day sampling period stream depth, width and volume at the primary S1 study segment ranged from to 0.0 to 0.3 m, 0.0 to 1.4 m and 0.0 to 7.1 m^3 . The minimum depth of the water table below the level of the streambed was -0.23 m occurring on the final day of the second, longer dry-cycle. pH ranged from 4.57 to 7.15 and was typically neutral

during rainfall trending to acidic post-stormflow, exhibiting a significant negative relationship with $[\text{CO}_2^*]$ ($r^2 = 0.78$, $n = 26$, $p < 0.05$). The measured ambient atmospheric and water temperatures ranged from 2.0 to 30.9 °C and 3.9 to 20.4 °C, with maximum 36-h range in variability of up to 23.1 and 9.8 °C, respectively. Rainfall intensity ranged from 0.0 to 77.8 mm h^{-1} with a daily mean of $0.7 \pm 0.9 \text{ mm h}^{-1}$ ($\pm\text{SD}$ herein) (Supplementary Table A1 and A2).

Dissolved gas concentrations and net fluxes

In situ water column excess CO_2 at the upstream S1 timeseries station fluctuated over two orders of magnitude from -11 to $1600 \text{ } \mu\text{M}$ ($289\text{--}30,800 \text{ } \mu\text{atm } p\text{CO}_2$), with a daily mean of $756 \pm 427 \text{ } \mu\text{M}$ ($15,300 \pm 8380 \text{ } \mu\text{atm}$; Fig. 2). Concentrations decreased towards atmospheric equilibrium during stormflow. Undersaturation was evident only during a hailstorm event that occurred at the onset of the initial wet-cycle, coinciding with the temperature-dependent CO_2 solubility maxima ($0.067 \text{ mol L}^{-1} \text{ atm}^{-1}$). The diel evolution of dissolved oxygen concentrations with respect to atmospheric equilibrium increased over the duration the wet cycles, with AOU ranging from -177 to $323 \text{ } \mu\text{M}$ (daily mean, $106 \pm 86 \text{ } \mu\text{M}$; Figs. 2, 3). Daily $\Delta[\text{CO}_2]$ was consistently greater than $\Delta[\text{O}_2]$ by a factor of 1.5 to 4.7, with both variables exhibiting a linear increase over time throughout the initial, longer wet-cycle ($r^2 = 0.84$ and 0.87 , respectively, $n = 12$, $p < 0.05$; Fig. 4) indicating net production of CO_2 via both in-stream processes and hyporheic exchange.

Over the 2 days of spatial sampling between-site variability in excess CO_2 within the 100 m study segment ranged up to $1200 \text{ } \mu\text{M}$ ($23,900 \text{ } \mu\text{atm}$; with samples collected at the same stage height and time of day). The highest excess CO_2 concentrations occurred at the S3 station, situated at the inlet of the man-made peat swamp channel at $1390 \pm 227 \text{ } \mu\text{M}$ ($28,400 \pm 4720 \text{ } \mu\text{atm}$; Table 1). The less-frequently inundated upstream sites with vegetation exhibited the greatest excess CO_2 variability between wet-cycles (S1 and S2, 700 and 550 μM , respectively), whereas the more-frequently inundated downstream sites that were void of vegetation were least variable (S3–S5, 322, 86 and 45 μM , respectively).

Excluding the influence of rainfall-induced turbulence and based on temporal changes in concentrations alone, the measured instantaneous diffusive water–air $\text{CO}_2\text{--C}$

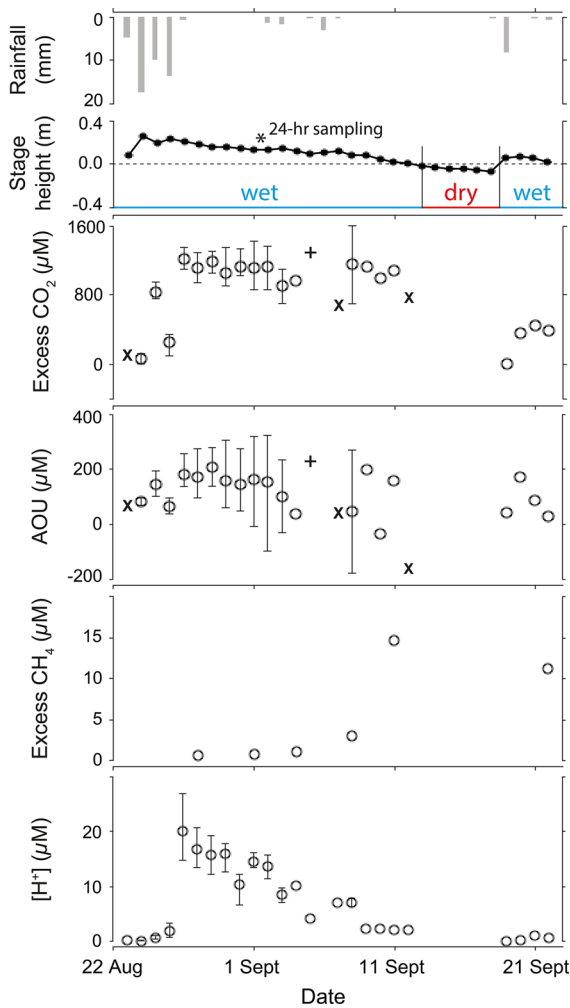


Fig. 2 Time series measurements of excess CO₂, AOU, excess CH₄ and [H⁺] taken over the initial two wet-cycles at the S1 study segment. Where $n \geq 2$, error bars indicate the range for each variable. Where $n = 1$, plus indicates samples collected between 06:00 and 10:00 h, circle indicates samples collected between 10:00 and 12:30 h, and cross indicates samples collected between 12:30 and 19:00 h

fluxes ranged from 11 to 80 mmol m⁻² day⁻¹ (mean, 45 ± 28 mmol m⁻² day⁻¹; $n = 6$). Measurements of the gas transfer velocity (k_{600}) averaged 0.26 ± 0.10 m day⁻¹, decreasing twofold at the S1 timeseries station during the initial wet-cycle from 0.33 to 0.16 m day⁻¹. Applying the average k -value obtained from all chamber measurements, instantaneous diffusive water–air CO₂–C fluxes ranged from –1 to 78 mmol m⁻² day⁻¹ (mean, 37 ± 21 mmol m⁻² day⁻¹; $n = 59$; Fig. 5). The measured instantaneous inter-site spatial variability in water–air CO₂–C fluxes

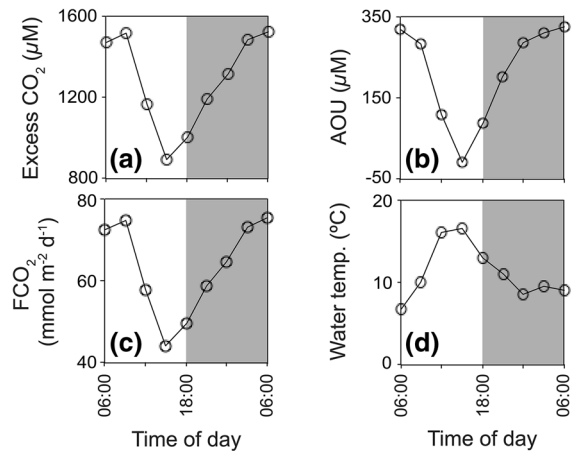


Fig. 3 Diel measurements of **a** excess CO₂, **b** the apparent oxygen utilisation (AOU), **c** the CO₂–C flux rate, and **d** water temperature at the S1 study segment during a period of low stage height, 10 days post-rewetting

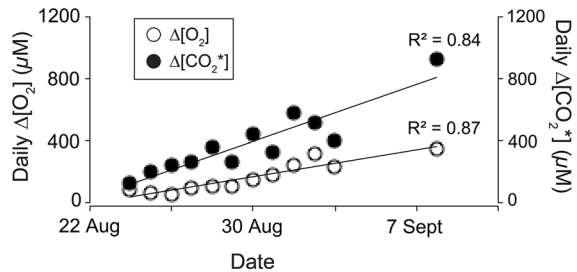


Fig. 4 Time series of daily change in concentration (Δ) for [O₂] and [CO₂*] taken at the S1 timeseries station during the initial, longer wet-to-dry cycle

ranged up to 76 mmol m⁻² day⁻¹, being similar in magnitude to the in situ temporal variability observed at the S1 timeseries station.

The influence of rainfall on k and CO₂–C fluxes during hydrologic transitions was calculated in this study via empirical equations. Considering only occasions influenced by precipitation >1 mm ($n = 9$ days), instantaneous k_{600} (HO) values ranged from 0.22 to 10.72 m day⁻¹, with a daily mean of 0.38 ± 0.17 m day⁻¹. Corresponding CO₂–C fluxes ranged from 0 to 567 mmol m⁻² day⁻¹, with a daily mean of 26 ± 23 mmol m⁻² day⁻¹. Considering only occasions with flow velocities ≥0.05 m s⁻¹ ($n = 9$ days), the slope-velocity parameterisation of Raymond et al. (2012) produced k_{600} values ranging from 0.27 to 1.40 m day⁻¹, with a daily mean of 0.53 ± 0.39 m day⁻¹. The corresponding CO₂–C fluxes on these occasions ranged from –3 to

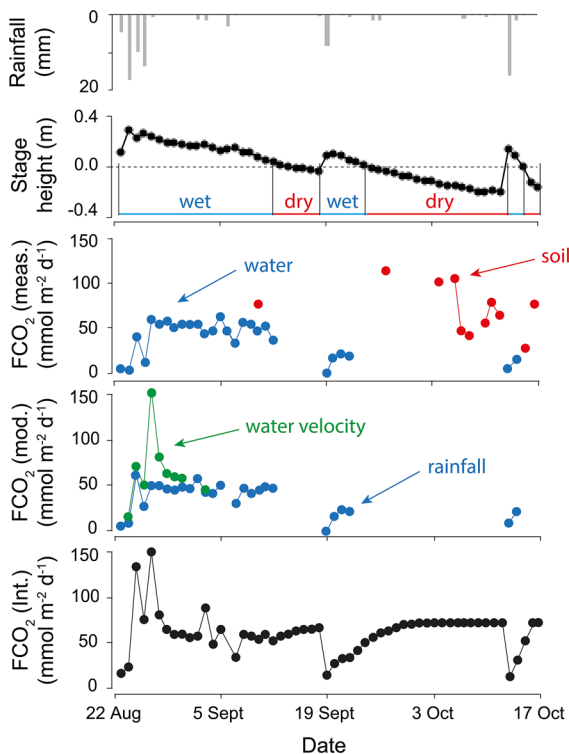


Fig. 5 Time series measurements of mean daily rainfall and stage height, measured and modelled $\text{CO}_2\text{-C}$ fluxes, as well as integrated water- and soil-air fluxes

$173 \text{ mmol m}^{-2} \text{ day}^{-1}$, with a daily mean of $67 \pm 38 \text{ mmol m}^{-2} \text{ day}^{-1}$ (Fig. 5; Supplementary Table A3). The influences of boundary layer condition on gas transfer velocities from both direct (e.g., rainfall) and indirect disturbance (e.g., changes to stream turbulence) may be approximately linearly additive, as with rainfall and wind speed (Ho et al. 2007). Under this assumption, the mean daily evasion rate during rainfall-induced hydrologic transitions was ~ 2 times higher than the mean background flux rate determined using floating chambers during still waters (59 ± 46 and $33 \pm 24 \text{ mmol m}^{-2} \text{ day}^{-1}$, respectively).

Integrated water- and soil-air fluxes

The measured daily mean $\text{CO}_2\text{-C}$ evasion rate from dry portions of the streambed was $72 \pm 27 \text{ mmol m}^{-2} \text{ day}^{-1}$ (range $27\text{--}115 \text{ mmol m}^{-2} \text{ day}^{-1}$), and was $\sim 20\%$ higher than the calculated mean daily water-air evasion rate encompassing changes from lotic to lentic waters. The peak-

measured soil-air efflux occurred 4-days after the onset of the second, longer dry-cycle when the mean stage height was -0.06 m . Factored for temporal changes to the water/soil ratio, the $[\text{CO}_2^*]$ saturation status, and water-air boundary layer condition over time the integrated daily mean flux of $\text{CO}_2\text{-C}$ from the S1 study segment was $61 \pm 24 \text{ mmol m}^{-2} \text{ day}^{-1}$ (range $12\text{--}156 \text{ mmol m}^{-2} \text{ day}^{-1}$; Fig. 5). This analysis employs the mean soil CO_2 flux obtained from all measurements to fill data gaps, thus assuming inhomogeneity throughout the streambed with progressive drying due to variable negative stage height and subsurface oxygen dynamics, and, that the mean soil CO_2 flux rate represents the average of all partial fluxes.

Water column excess CH_4 and net fluxes

Excess CH_4 increased from 0.6 to $14.6 \mu\text{M}$ ($349\text{--}8700 \mu\text{atm } p\text{CH}_4$) at the S1 station over the initial wet-cycle, with a median concentration of $2.1 \mu\text{M}$ ($1200 \mu\text{atm}$) and median calculated background $\text{CH}_4\text{-C}$ evasion rate of $0.3 \text{ mmol m}^{-2} \text{ day}^{-1}$ (range $0.1\text{--}1.9 \text{ mmol m}^{-2} \text{ day}^{-1}$). The maximum water column CH_4 concentrations occurred towards the end of the initial, longer wet-cycle (Fig. 2). Spatial variability in excess CH_4 ranged from 0.4 to $12.9 \mu\text{M}$ ($239\text{--}7940 \mu\text{atm}$), with resultant background water-air $\text{CH}_4\text{-C}$ evasion rates ranging from 0.1 to $1.7 \text{ mmol m}^{-2} \text{ day}^{-1}$ (overall mean, $0.7 \pm 0.6 \text{ mmol m}^{-2} \text{ day}^{-1}$).

Wet and dry cycle dynamics

A decrease in wet-cycle duration (T_W) coincided with a decrease in daily mean water column excess CO_2

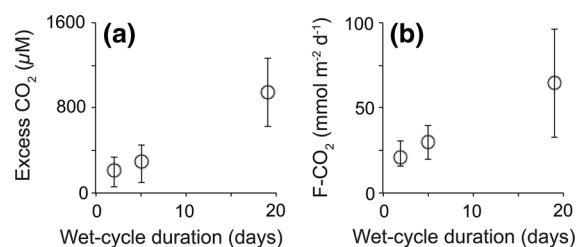


Fig. 6 The relationship between wet-cycle duration and **a** mean daily water column excess CO_2 concentrations, as well as **b** integrated water and soil-air $\text{CO}_2\text{-C}$ fluxes. Error bars indicate the standard deviations for each cycle

concentrations (wet-cycle 1–3, 949 ± 322 , 298 ± 203 and 213 ± 155 μM ; $T_w = 19, 5$ and 2 d, respectively, $r^2 = 0.99$, $p < 0.05$; Fig. 6a) and integrated water and soil–air CO_2 –C evasion rates (wet-cycle 1–3, 65 ± 32 , 30 ± 10 , and 21 ± 14 $\text{mmol m}^{-2} \text{day}^{-1}$, respectively; Fig. 6b). Stage height correlated significantly with daily evapotranspiration rate ($r^2 = 0.49$, $n = 56$, $p < 0.05$), daily $\Delta[\text{CO}_2]$ and $\Delta[\text{O}_2]$ (wet-cycle 1, $r^2 = 0.73$ and 0.77 , respectively, $n = 12$, $p < 0.05$), water/soil ratio-corrected fluxes (water, $r^2 = 0.52$; soil, $r^2 = 0.93$; $p < 0.05$; Fig. 7), as well as with water temperature ($r^2 = 0.23$; $p < 0.05$).

Discussion

Water–air versus soil–air exchange

Our results from an intermittent stream supports recent research from seasonally ephemeral aquatic systems which show that mean soil–air CO_2 –C fluxes typically exceed those from the same watercourses when inundated (Table 2). Based on in situ measurements

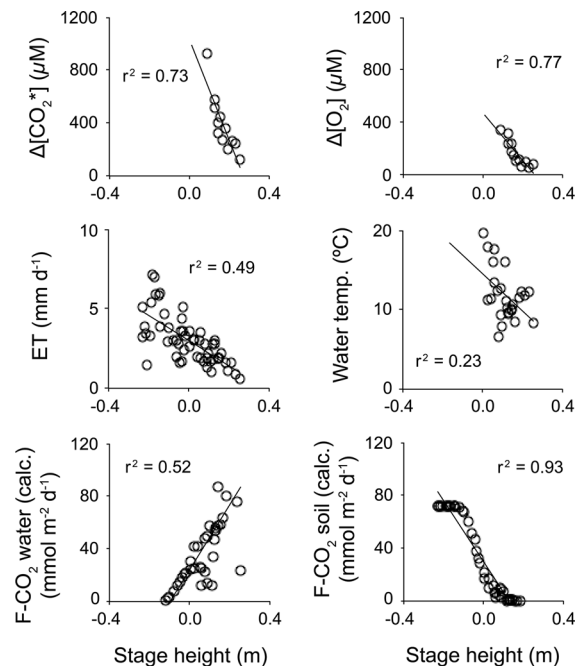


Fig. 7 Relationships between mean stage height with $\Delta[\text{CO}_2^*]$, $\Delta[\text{O}_2]$, evapotranspiration rate (ET), water temperature, as well as the calculated total water and soil ratio-corrected CO_2 –C fluxes per daily time step at the S1 study site

when the stream study sites were disconnected, the contributions of soil–air CO_2 –C fluxes at the S1 timeseries station exceeded water–air fluxes by a factor of ~ 2 . However, this does not account for changes to the emerged/submerged area over time, or to stream flow dynamics during dry-to-wet and baseflow-stormflow hydrologic transitions. In the case of the upper Jamison Creek watercourse, integrating these factors into the analyses produced contrasting results; with the contributions of water- and soil–air evasion to total CO_2 –C fluxes being approximately equal (43 and 40 mol, respectively).

System-specific dissimilarities in wet and dry cycle intermittence in this study influenced areal water–soil distributions, spatial flux dynamics, and, consequently, the relative magnitude of total C-gas fluxes. Further, antecedent soil moisture conditions linked to the length of the preceding dry-cycle and consequent negative stage height influences the duration of each rewetting-cycle (Mohanty et al. 2015) and nutrient hydrochemistry (Biron et al. 1999), in conjunction with prevailing meteorological conditions (e.g. rain event intensity and duration; percent cloud cover). Considering this, we hypothesise that GHG fluxes in frequently intermittent watercourses are likely to display contrasting characteristics to seasonally ephemeral watercourses over annual time scales. Accordingly, it may prove more accurate to apply a distinction between the wet and dry fraction periods of seasonally ephemeral watercourses (typically dry for months at a time) and other more frequently intermittent aquatic systems (wet and dry cycles ranging from days to weeks) for the future integration of non-perennial fluvial systems into global carbon budget models.

The rates of GHG evasion from low-order streams can be disproportionately high in magnitude compared to other fluvial systems of the lower catchment, with a general trend of decreasing gas transfer velocities and $p\text{CO}_2$ with increasing stream order (Butman and Raymond 2011). For example, in a paraglacial mixed forest watershed (Québec, Canada), the smallest first-order streams represented $<20\%$ of the total river network surface and contributed $>35\%$ of the total fluvial GHG emissions (Campeau et al. 2014). The CO_2 evasion rates reported for an intermittent watercourse in this study and reported for both wet and dry cycles in seasonally ephemeral watercourses in semi-arid environments (von Schiller et al. 2014; Gómez-

Table 2 Comparison summary of mean CO₂ concentration and fluxes for temporary ponds, perennial flowing rivers and streams, seasonally ephemeral watercourses, lakes, and wetlands worldwide (\pm SD; ranges shown in parentheses)

Location/watercourse type	Flux wet ^f (mmol m ⁻² day ⁻¹)	Flux wet ^s (mmol m ⁻² day ⁻¹)	Flux dry (mmol m ⁻² day ⁻¹)	References
River Fluvià, Spain/seasonally ephemeral	22* (11–26)	7* (6–11)	58* (10–124)	von Schiller et al. (2014)
Iberia, Spain/seasonally ephemeral	83 \pm 56	–	213 \pm 106 (93–418)	Gómez-Gener et al. (2016)
Tucson, Arizona/seasonally ephemeral	–	–	44 \pm 8 ^{p,se,v} (20–3173)	Gallo et al. (2014)
Worldwide/small ponds << 0.001 km ²	–	35 \pm 5 ^{m,se}	–	Holgerson and Raymond (2016)
Mediterranean/temporary ponds	–	3 (1–11)	(2–96) ^v	Catalán et al. (2014)
Worldwide/flowing waters	766 ^m	–	–	Raymond et al. (2013)
Conterminous USA/flowing waters	541 \pm 182 ^m (201–914)	–	–	Butman and Raymond (2011)
Boreal/lakes	–	33 ^m	–	Weyhenmeyer et al. (2015)
Worldwide/lakes and reservoirs	–	7 ^m (1–17)	–	Raymond et al. (2013)
Tropical/wetlands [†]	–	107 \pm 50 ^{p,v} (20–141)	255 \pm 111 ^{p,v} (69–493)	Sjögersten et al. (2014, Table 4)
Boreal/fen ^{††}	–	117 ^{p,v}	144 ^{p,v}	Sonnentag et al. (2010)
This study	67 \pm 38 ^m (–9 to 349)	30 \pm 20 (0–62)	72 \pm 27 ^v (27–115)	

^f Flowing waters. ^s Stagnant waters. ^m Modelled fluxes. * Median values. ^{se} \pm Standard error. ^v Includes vegetated and/or non-vegetated soils. ^p Considers partial soil rewetting and/or fluctuating water table depth, typically <0 m. [†] Excludes floodplains. ^{††} Considers fluxes during the snow-free period

Gener et al. 2016), are typically lower than evasion rates reported for perennial flowing waters (Butman and Raymond 2011; Raymond et al. 2013) and are more similar to evasion rates reported for still waters (Raymond et al. 2013; Catalán et al. 2014; Weyhenmeyer et al. 2015; Holgerson and Raymond 2016) and wetlands (Sonnentag et al. 2010; Sjögersten et al. 2014) (Table 2).

'Hot' and 'cold' phenomena in C-gas evasion cycle

Spatial and temporal patterns in stream hydrologic status alter biotic assemblage composition and ecosystem metabolism (Hall et al. 2015; Sabater et al. 2016), nutrient biogeochemistry (Birch 1958; Mohanty et al. 2015), soil diffusivity (Davidson and Janssens 2006), benthic redox dynamics (Harrison et al. 2005; Knorr

et al. 2009; Gallo et al. 2014), as well as dissolved organic matter composition and lability (Buffam et al. 2001; Raymond and Saiers 2010; Jeanneau et al. 2015). Such changes can drive spatially variable 'hot' and 'cold' moments in the dry-wet-dry C-gas evasion cycle (i.e., increased and decreased fluxes, respectively; McClain et al. 2003). For example, in urbanized ephemeral waterways in Arizona, USA Gallo et al. (2014) found CO₂-C emissions to increase following temporary rewetting of the dry streambed sediments (soil moisture content $\leq 18 \pm 3\%$ and $t \leq 6$ -h; pre-wetting, 65 ± 53 mmol m⁻² day⁻¹; post-wetting peak, 706 ± 453 mmol m⁻² day⁻¹; sandy-loam soil group); with the flux magnitude correlated to soil moisture status. Our soil chamber measurements did not detect a notable increase in dry-cycle soil fluxes following partial rewetting. However, the empirical modelling presented herein considering

complete cycles of inundation and emersion (e.g., stage height during rewetting >0 m; $T_W = >1$ days), demonstrated that intense physical forcing by transient meteorological events can also produce further hydrologically mediated ‘hot moment’ phenomena during which water–air fluxes can equal or exceed soil fluxes.

Of the two models used to calculate the influence of environmental variables on the rates of water–air CO_2 –C fluxes, we found the parameterisation given by Ho et al. (1997) to closely approximate the mean background water column gas transfer velocities as determined from floating chamber measurements (when $R_n = 0.00 \text{ mm h}^{-1}$, k_{600} (HO) = 0.22 m day^{-1} ; mean chamber-derived k_{600} in this study, $0.26 \pm 0.10 \text{ m day}^{-1}$). The Ho et al. (1997) model was developed using sulphur hexafluoride (SF_6) tracer injections in a closed system and incorporated the kinematic energy flux of natural raindrop size distributions, which monotonically decreases as raindrop size decreases (Marshall and Palmer 1948). Incorporating the influence of physical forcing by precipitation at the water–air boundary layer during hydrologic phase transitions, this parameterisation increases our mean daily background fluxes of CO_2 –C on days influenced by rainfall by 30%, with the maximum instantaneous evasion rate of $567 \text{ mmol m}^{-2} \text{ day}^{-1}$ being 5 times higher than our measured peak post-wet-cycle soil flux rate of $115 \text{ mmol m}^{-2} \text{ day}^{-1}$.

The effect of precipitation on evasion is most pronounced where wind velocity does not dominate turbulence-driven C-gas exchange in limnological systems such as small ponds (Ho et al. 1997; Vachon and Prairie 2013). In this study, hydrophobic macromolecular surfactants (personal observations) may have diminished the kinematic energy flux produced by boundary layer raindrop penetration (e.g. Frew et al. 1990, 2004; McKenna and McGillis 2004), as evidenced by the 47% decrease in measured k_{600} over the initial wet-cycle. As time progresses since rewetting, so does the thickness and extent of surfactants. This in turn limits the transfer of gases, reducing water column reaeration capacity and engendering an accumulation of CO_2 (e.g., Fig. 6a). Importantly, the presence of surfactants would most likely inhibit C-gas evasion rates during precipitation events that occur throughout the later term of a phytoplankton-dominated wet-cycle, prior to flushing of the system by significant rainfall.

Under low-flow conditions, the slope-depth-velocity parameterisation of Raymond et al. (2012) also provided a reasonable approximation of the gas transfer velocities determined from our chamber measurements (mean k_{600} difference, $\pm 0.1 \text{ m day}^{-1}$). This model was formulated from 563 purposeful tracer experiments in running waters of varying stream order and flow conditions. Overall, k_{600} (RAY) was 2.1 times greater than our measured gas transfer velocities, with the discrepancy between measured and modelled k_{600} being due to the exclusion of higher flow velocities by our chamber measurements (e.g. because of inherent limitations of using floating chambers to determine k in running waters; Kremer et al. 2003; Lorke et al. 2015). Inclusive of the influence of stream hydraulics, this parameterisation increases our mean daily background CO_2 –C fluxes on occasions with flow velocities $>0.05 \text{ m s}^{-1}$ by 60%, with a maximum increase of $108 \text{ mmol m}^{-2} \text{ day}^{-1}$ (163%) on the first day of the initial wet-cycle post-rainfall, coinciding with a subsidence in stormflow and concurrent increase in excess CO_2 concentrations.

For both measured and modelled fluxes, CO_2 degassing from the S1 segment ceased during periods of heavy rainfall when aqueous $[\text{CO}_2^*]$ approached atmospheric equilibrium, as well as during the initial hailstorm event when there was a short 2-h period of net influx of CO_2 due to rapid cooling of the water and a subsequent increase in CO_2 solubility. During storm events, such equilibrium and undersaturation states in typically supersaturated aquatic systems may also be preceded by a pulse of elevated CO_2 degassing relative to baseflow rates (Looman et al. 2016), as increased streamwater velocity increases the gas transfer velocity due to higher streambed-generated shear stress (Beaulieu et al. 2012). The precipitation-induced dilution effect may then be succeeded by an increase in water column $[\text{CO}_2^*]$ derived from soil respiration, transported by the migration of surface waters infiltrating through groundwater pathways (Johnson et al. 2007, 2008; Dinsmore et al. 2013). Thus, the combined influence on water–air gas exchange rates of rainfall induced changes in gas transfer velocity as well as CO_2^* concentration-discharge hysteresis patterns is temporally erratic.

Overall, dry-to-wet and baseflow-stormflow hydrological transitions represented 25% of wet-cycle days yet contributed 42% of total water–air CO_2 –C

emissions. Evasion rates were lowest on rewetting days with precipitation >10 mm, with such cold moments decreasing fluxes by up to 100% with respect to mean non-transition phase water–air fluxes (average decrease of 20%). Conversely, fluxes were increased by an average of 12% on days with precipitation ranging from 1 to 10 mm and by 20% on days with precipitation <1 mm. Regarding the latter, this increase is primarily attributable to residual post-rainfall flow velocities of up to 0.1 m s^{-1} compared to those fluxes occurring in otherwise still waters. Accordingly, the maximal water–air CO_2 flux potential in the present study occurred as a result of short-term physical forcing by rainfall when the streambed was previously inundated and not necessarily during peak partial pressures as might otherwise be expected. Importantly, the degree of misinterpretation for total water–air CO_2 flux accounting if non-continuous sampling methods are employed would be site-specific, and would be largely dependent upon the $p\text{CO}_2$ status; the frequency, duration and magnitude of rainfall events; relative changes to the streambed water/soil ratio during hydrologic phase transitions; and, moreover, the timing and frequency that periodic samples are taken. We highlight that additional studies are required for these findings to be generalised to other catchments.

The contribution of methane

The sustained global warming potential (SGWP; Neubauer and Megonigal 2015) of mean daily water–air CH_4 contributions to total C-gas emissions from the S1 study segment—expressed as CO_2 equivalents—were similar to the SGWPs of mean soil CO_2 emissions over a 20-year time frame and to measured background water–air emissions over a 100-year time frame (76 ± 67 and $36 \pm 25 \text{ mmol m}^{-2} \text{ day}^{-1} \text{ CO}_2$ equivalents, respectively). As we only considered diffusive CH_4 fluxes in this study, additional contributions via the ebullition pathway (e.g., Prairie and del Giorgio 2013) would likely extend the contributions of CH_4 fluxes to total C-gas emissions from the S1 study segment to beyond those of CO_2 from both the soil- and water–air interfaces over the 20 and 100-year time frames, respectively.

The maximum water column excess CH_4 concentrations in the present study occurred during the final time period of the initial 21-day wet-cycle (Fig. 2), akin to the observed trends in CO_2 . Low nocturnal

dissolved oxygen saturations that occurred post-wetting ($25 \pm 6\%$ saturation) might have facilitated anaerobic metabolism and methane production. The hyporheic zone of the streambed represents the interface between ground and surface waters and is a dynamic ecotone for microbial metabolism (Claret and Boulton 2009), with the degradation of organic matter in surface sediments causing localised oxygen depletions. As well as the traditional pathway of microbial anaerobic methanogenesis, CH_4 production can also occur in oxic waters via acetoclastic methanogenesis, driven by algal dynamics (Bogard et al. 2014). CO_2 can be produced in turn by the oxidation of methane, both aerobically and anaerobically (Thauer et al. 2008). Thus, although stoichiometric analyses of the biogeochemical drivers of CH_4 dynamics were beyond the specific aims of the present study the temporal changes for trends in AOU and excess CO_2 , as well as a significant negative relationship between excess CH_4 and $[\text{H}^+]$ ($r^2 = 0.78$; $p < 0.05$), suggest that successions in microbial and algal community composition may be responsible for an increase in CH_4 production over longer-duration wet-cycles. Such potential competitive exclusion processes most likely occur in conjunction with post-rewetting redox oscillations of oxidised iron and sulphate substrate available for anaerobic metabolism (Knorr et al. 2009). Additionally, correlations between excess CH_4 and both ambient atmospheric and water temperatures ($r^2 = 0.67$ and 0.31 , respectively, $p < 0.05$) and water temperature with $\text{CH}_4:\text{CO}_2$ ratio ($r^2 = 0.83$; $p < 0.05$) indicate that methanogenesis may be temperature dependent over short time scales, and reflect the physiological kinetic processes generating these fluxes (see Yvon-Durocher et al. 2014).

Conclusions and implications

Our observations demonstrate that wet and dry cycle periodicity, redox processes, atmospheric forcing by rainfall, site-specific ephemerality, and small-scale spatial heterogeneity were key influential factors in controlling C-gas flux rates in the upper Jamison Creek watercourse. In non-perennial watercourses maximal and minimal fluxes may occur during hydrologic phase transitions, and, although short-lived and problematic to quantify at larger regional scales, such hot and cold moments may comprise an appreciable component of

the local and regional carbon budgets for aquatic systems. Up to 75% of watercourses in Australia are ephemeral (Sheldon et al. 2010) and these non-perennial watercourses are currently excluded from Australia's carbon accounting estimates (Haverd et al. 2013; Poulter et al. 2014). Therefore, due to the high rate of emissions from dry watercourses, as well as fluctuant nature in the rate of emissions during and following complete or partial rewetting, the overall relative magnitude of this continental carbon sink and that of other semi-arid ecosystems of the southern hemisphere may be misrepresented.

Acknowledgements Special thanks are given to V. Kumar and C. Barton of Western Sydney University (UWS), the Blue Mountains City Council (BMCC), C. Holloway (SCU), and W. Davis for their assistance with logistics. We acknowledge funding from the Australian Research Council (LE120100156, DE140101733 and DE150100581).

Compliance with ethical standards

Conflict of interest The authors declare that they have no conflict of interest.

References

- Alin SR, Rasera MF, Salimon CI, Richey EJ, Holtgrieve GW, Krusche AV, Snidvongs A (2011) Physical controls on carbon dioxide transfer velocity and flux in low-gradient river systems and implications for regional carbon budgets. *J Geophys Res* 116:G01009
- Bakker DC, Bange HW, Gruber N (2014) Air–sea interactions of natural long-lived greenhouse gases (CO₂, N₂O, CH₄) in a changing climate. In: Liss PS, Johnson MT (eds) *Ocean–atmosphere interactions of gases and particles*. Springer Earth System Sciences, New York
- Bass AM, Munksgaard NC, Leblanc M, Tweed S, Bird MI (2014) Contrasting carbon export dynamics of human impacted and pristine tropical catchments in response to a short-lived discharge event. *Hydrol Process* 28:1835–1843
- Battin TJ, Luyssaert S, Kaplan LA, Aufdenkampe AK, Richter A, Tranvik LJ (2009) The boundless carbon cycle. *Nat Geosci* 2:598–600
- Beaulieu JJ, Shuster WD, Rebholz JA (2012) Controls on gas transfer velocities in a large river. *J Geophys Res Biogeosci* 117:G02007
- Bernal S, Schiller D, Sabater F, Martí E (2012) Hydrological extremes modulate nutrient dynamics in Mediterranean climate streams across different spatial scales. *Hydrobiologia* 719:31–42
- Bernot MJ, Sobota DJ, Hall RO et al (2010) Inter-regional comparison of land-use effects on stream metabolism. *Freshw Biol* 55:1874–1890
- Birch HF (1958) The effect of soil drying on humus decomposition and nitrogen availability. *Plant Soil* 10:9–31
- Biron PM, Roy AG, Courschesne F, Hendershot WH, Côté B, Fyles J (1999) The effects of antecedent moisture conditions on the relationship of hydrology to hydrochemistry in a small forested watershed. *Hydrol Process* 13:1541–1555
- Bogard MJ, del Giorgio PA, Boutet L et al (2014) Oxidic water column methanogenesis as a major component of aquatic CH₄ fluxes. *Nat Commun* 5:5350
- Borges AV, Darchambeau F, Teodoru CR et al (2015) Globally significant greenhouse-gas emissions from African inland waters. *Nat Geosci* 8:637–642
- Buffam I, Galloway JN, Blum LK, McGlathery KJ (2001) A stormflow/baseflow comparison of dissolved organic matter concentrations and bioavailability in an Appalachian stream. *Biogeochemistry* 53:269–306
- Bureau of Meteorology (BoM) (2015a) Climate data online. Australian Government Bureau of Meteorology. http://www.bom.gov.au/climate/averages/tables/cw_063039.shtml. Accessed 26 Oct 2015
- Bureau of Meteorology (BoM) (2015b) Climate data online. Australian Government Bureau of Meteorology. <http://www.bom.gov.au/watl/eto/>. Accessed 26 Oct 2015
- Butman D, Raymond PA (2011) Significant efflux of carbon dioxide from streams and rivers in the United States. *Nat Geosci* 4:839–842
- Campeau A, Lapierre J, Vachon D, del Giorgio PA (2014) Regional contribution of CO₂ and CH₄ fluxes from the fluvial network in a lowland boreal landscape of Québec. *Glob Biogeochem Cycle* 28:1–13
- Casas-Ruiz JP, Tittel J, von Schiller D (2016) Drought-induced discontinuities in the source and degradation of dissolved organic matter in a Mediterranean river. *Biogeochemistry* 127:125–139
- Catalán N, von Schiller D, Marcé R, Koschorreck M, Gómez-Gener L, Obrador B (2014) Carbon dioxide efflux during the flooding phase of temporary ponds. *Limnetica* 33:349–360
- Claret C, Boulton A (2009) Integrating hydraulic conductivity with biogeochemical gradients and microbial activity along river–groundwater exchange zones in a subtropical stream. *Hydrogeol J* 17:151–160
- Costigan KH, Daniels MD, Dodds WK (2015) Fundamental spatial and temporal disconnections in the hydrology of an intermittent prairie headwater network. *J Hydrol* 522:305–316
- Crusius J, Wanninkhof R (2003) Gas transfer velocities measured at low wind speed over a lake. *Limnol Oceanogr* 48:1010–1017
- Datry T, Larned ST, Tockner K (2014) Intermittent rivers: a challenge for freshwater ecology. *Bioscience* 64:229–235
- Davidson EA, Janssens IA (2006) Temperature sensitivity of soil carbon decomposition and feedbacks to climate change. *Nature* 440:165–173
- Dieter D, von Schiller D, García-Roger EM et al (2011) Pre-conditioning effects of intermittent stream flow on leaf litter decomposition. *Aquat Sci* 73:599–609
- Dinsmore KJ, Billett MF (2008) Continuous measurement and modeling of CO₂ losses from a peatland stream during stormflow events. *Water Resour Res* 44:W12417

- Dinsmore KJ, Wallin MB, Johnson MS, Billett MF, Bishop K, Pumpanen J, Ojala A (2013) Contrasting CO₂ concentration discharge dynamics in headwater streams: a multi-catchment comparison. *J Geophys Res Biogeosci* 118:445–461
- Dodds WK (2006) Eutrophication and trophic state in rivers and streams. *Limnol Oceanogr* 51:671–680
- Dodds WK, Perkin JS, Gerken JE (2013) Human impact on freshwater ecosystem services: a global perspective. *Environ Sci Technol* 47:9061–9068
- Fazi S, Vazquez E, Casamayor EO, Amalfitano S, Butturini A (2013) Stream hydrological fragmentation drives bacterioplankton community composition. *PLoS ONE* 8:e64109
- Frankignoulle M (1988) Field measurements of air-sea CO₂ exchange. *Limnol Oceanogr* 33:313–322
- Frew NM, Goldman JC, Dennett MR, Johnson AS (1990) Impact of phytoplankton-generated surfactants on air-sea gas exchange. *J Geophys Res* 95:3337–3352
- Frew NM, Bock EJ, Schimpf U et al (2004) Air-sea gas transfer: its dependence on wind stress, small-scale roughness, and surface films. *J Geophys Res* 109:C08S17
- Fryirs KA, Cowley K, Hose GC (2016) Intrinsic and extrinsic controls on the geomorphic condition of upland swamps in Eastern NSW. *Catena* 137:100–112
- Gallo EL, Lohse KA, Ferlin CM et al (2014) Physical and biological controls on trace gas fluxes in semi-arid urban ephemeral waterways. *Biogeochemistry* 121:189–207
- Godsey SE, Kirchner JW (2014) Dynamic, discontinuous stream networks: hydrologically driven variations in active drainage density, flowing channels and stream order. *Hydrol Process* 28:5791–5803
- Gómez-Gener L, Obrador B, Marcé R et al (2016) When water vanishes: magnitude and regulation of carbon dioxide emissions from dry temporary streams. *Ecosystems* 19:710–723
- Hagen EM, McTammany ME, Webster JR, Benfield EF (2010) Shifts in allochthonous input and autochthonous production in streams along an agricultural land-use gradient. *Hydrobiologia* 655:61–77
- Haines AT, Finlayson BL, McMahon TA (1988) A global classification of river regimes. *Appl Geogr* 8:255–272
- Hall RO, Yackulic CB, Kennedy TA et al (2015) Turbidity, light, temperature, and hydropeaking control primary productivity in the Colorado River, Grand Canyon. *Limnol Oceanogr* 60:512–526
- Hansen WF (2001) Identifying stream types and management implications. *For Ecol Manag* 143:39–46
- Harrison JA, Matson PA, Fendorf SE (2005) Effects of a diel oxygen cycle on nitrogen transformations and greenhouse gas emissions in a eutrophied subtropical stream. *Aquat Sci* 67:308–315
- Haverd V, Raupach MR, Briggs PR et al (2013) The Australian terrestrial carbon budget. *Biogeosciences* 10:851–869
- Ho DT, Bliven LF, Wanninkhof R, Schlosser P (1997) The effect of rain on air–water gas exchange. *Tellus B* 49:149–158
- Ho DT, Veron F, Harrison E, Bliven LF, Scott N, McGillis WR (2007) The combined effect of rain and wind on air–water gas exchange: a feasibility study. *J Mar Syst* 66:150–160
- Holgeron MA, Raymond PA (2016) Large contribution to inland water CO₂ and CH₄ emissions from very small ponds. *Nat Geosci* 9:222–226
- Holmes NT (1999) Recovery of headwater stream flora following the 1989–1992 groundwater drought. *Hydrol Process* 13:341–354
- Hook AM, Yeakley JA (2005) Stormflow dynamics of dissolved organic carbon and total dissolved nitrogen in a small urban watershed. *Biogeochemistry* 75:409–431
- Jähne B, Münnich K, Dutzi R, Huber W, Libner P (1987) On the parameters influencing air–water gas exchange. *J Geophys Res* 92:1937–1949
- Janke BD, Finlay JC, Hobbie SE, Baker LA, Sterner RW, Nidzgorski D, Wilson BN (2014) Contrasting influences of stormflow and baseflow pathways on nitrogen and phosphorus export from an urban watershed. *Biogeochemistry* 121:209–228
- Jeanneau L, Denis M, Pierson-Wickmann A, Gruau G, Lambert T, Petitjean P (2015) Sources of dissolved organic matter during storm and inter-storm conditions in a lowland headwater catchment: constraints from high-frequency molecular data. *Biogeosciences* 12:4333–4343
- Johnson MS, Weiler M, Couto EG, Riha SJ, Lehmann J (2007) Storm pulses of dissolved CO₂ in a forested headwater Amazonian stream explored using hydrograph separation. *Water Resour Res* 43:W11201
- Johnson MS, Lehmann J, Riha SJ, Krusche AV, Richey JE, Ometto JP, Couto EG (2008) CO₂ efflux from Amazonian headwater streams represents a significant fate for deep soil respiration. *Geophys Res Lett* 35:L17401
- Jones JB, Mulholland PJ (1998) Carbon dioxide variation in a hardwood forest stream: an integrative measure of whole catchment soil respiration. *Ecosystems* 1:183–196
- Knorr KH, Lischeid G, Blodau C (2009) Dynamics of redox processes in a minerotrophic fen exposed to a water table manipulation. *Geoderma* 153:379–392
- Koprivnjak JF, Dillon PJ, Molot LA (2010) Importance of CO₂ evasion from small boreal streams. *Glob Biogeochem Cycle* 24:GB4003
- Kremer J, Nixon S, Buckley B, Roques P (2003) Technical note: conditions for using the floating chamber method to estimate air–water gas exchange. *Estuar Coast* 26:985–990
- Larned ST, Datry T, Arscott DB, Tockner K (2010) Emerging concepts in temporary-river ecology. *Freshw Biol* 55:717–738
- Leopold LB, Maddock T (1953) The hydraulic geometry of stream channels and some physiographic implications. United States Geological Survey, Reston, pp 1–57
- Looman A, Santos IR, Tait DR, Webb JR, Sullivan CA, Maher DT (2016) Carbon cycling and exports over diel and flood-recovery timescales in a subtropical rainforest headwater stream. *Sci Total Environ* 550:645–657
- Lorke A, Bodmer P, Noss C et al (2015) Technical note: drifting versus anchored flux chambers for measuring greenhouse gas emissions from running waters. *Biogeosciences* 12:7013–7024
- Marshall JS, Palmer WM (1948) The distribution of raindrops with size. *J Meteorol* 5:165–166
- McClain ME, Boyer EW, Dent CL et al (2003) Biogeochemical hot spots and hot moments at the interface of terrestrial and aquatic ecosystems. *Ecosystems* 6:301–312
- McKenna SP, McGillis WR (2004) The role of free-surface turbulence and surfactants in air–water gas transfer. *Int J Heat Mass Transf* 47:539–553

- McMahon TA, Finlayson BL (2003) Droughts and anti-droughts: the low flow hydrology of Australian rivers. *Freshw Biol* 48:1147–1160
- Millero FJ (2007) The marine inorganic carbon cycle. *Chem Rev* 107:308–341
- Mohanty SK, Saiers JE, Ryan JN (2015) Colloid mobilization in a fractured soil during dry-wet cycles: role of drying duration and flow path permeability. *Environ Sci Technol* 49:9100–9106
- Nadeau TL, Rains MC (2007) Hydrological connectivity between headwater streams and downstream waters: how science can inform policy. *J Am Water Resour Assoc* 43:118–133
- Neubauer SC, Megonigal JP (2015) Moving beyond global warming potentials to quantify the climatic role of ecosystems. *Ecosystems* 18:1000–1013
- Palta MM, Ehrenfeld JG, Groffman PM (2014) “Hotspots” and “hot moments” of denitrification in urban brownfield wetlands. *Ecosystems* 17:1121–1137
- Peter H, Singer GA, Preiler C, Chiffard P, Stenciczka G, Battin TJ (2014) Scales and drivers of temporal $p\text{CO}_2$ dynamics in an Alpine stream. *J Geophys Res Biogeosci* 119:1078–1091
- Poulter B, Frank D, Ciais P et al (2014) Contribution of semi-arid ecosystems to interannual variability of the global carbon cycle. *Nature* 509:600–603
- Prairie YT, del Giorgio PA (2013) A new pathway of freshwater methane emissions and the putative importance of microbubbles. *Inland Waters* 3:311–320
- Raymond PA, Saiers JE (2010) Event controlled DOC export from forested watersheds. *Biogeochemistry* 100:197–209
- Raymond PA, Zappa CJ, Butman D et al (2012) Scaling the gas transfer velocity and hydraulic geometry in streams and small rivers. *Limnol Oceanogr Fluids Environ* 2:41–53
- Raymond PA, Hartmann J, Lauerwald R et al (2013) Global carbon dioxide emissions from inland waters. *Nature* 503:355–359
- Raymond PA, Saiers JE, Sobczak WV (2016) Hydrological and biogeochemical controls on watershed dissolved organic matter transport: pulse-shunt concept. *Ecology* 97(1):5–16
- Regnier P, Friedlingstein P, Ciais P et al (2013) Anthropogenic perturbation of the carbon fluxes from land to ocean. *Nat Geosci* 6:597–607
- Richey JE, Devol AH, Wofsy SC, Victoria R, Riberio MN (1988) Biogenic gases and the oxidation and reduction of carbon in Amazon River and floodplain waters. *Limnol Oceanogr* 33:551–561
- Rudorff CM, Melack JM, MacIntyre S, Barbosa CC, Novo EM (2011) Seasonal and spatial variability of CO_2 emission from a large floodplain lake in the lower Amazon. *J Geophys Res* 116:G04007
- Ruiz-Halpern S, Maher DT, Santos IR, Eyre BD (2015) High CO_2 evasion during floods in an Australian subtropical estuary downstream from a modified acidic floodplain wetland. *Limnol Oceanogr* 60:42–56
- Sabater S, Timoner X, Borrego C, Acuña V (2016) Stream biofilm responses to flow intermittency: from cells to ecosystems. *Front Environ Sci* 4:14. doi:10.3389/fenvs.2016.00014
- Sadat-Noori M, Maher DT, Santos IR (2015) Groundwater discharge as a source of dissolved carbon and greenhouse gases in a subtropical estuary. *Estuar Coast* 39:639–656
- Salemi LF, Groppo JD, Trevisan R, de Moraes JM, de Paula LW, Martinelli LA (2012) Riparian vegetation and water yield: a synthesis. *J Hydrol* 454–455:195–202
- Shaw JR, Cooper DJ (2008) Linkages among watersheds, stream reaches, and riparian vegetation in dryland ephemeral stream networks. *J Hydrol* 350:68–82
- Sheldon F, Bunn SE, Hughes JM, Arthington AH, Balcombe SR, Fellows CS (2010) Ecological roles and threats to aquatic refugia in arid landscapes: dryland river waterholes. *Mar Freshw Res* 61:885–895
- Sjögersten S, Black CR, Evers S, Hoyos-Santillan J, Wright EL, Turner BL (2014) Tropical wetlands: a missing link in the global carbon cycle? *Glob Biogeochem Cycle* 28:1371–1386
- Snelder TH, Datry T, Lamouroux N, Larned ST, Sauquet E, Pella H, Catalogne C (2013) Regionalization of patterns of flow intermittence from gauging station records. *Hydrol Earth Syst Sci* 17:2685–2699
- Sonnentag O, van der Kamp G, Barr AG, Chen JM (2010) On the relationship between water table depth and water vapor and carbon dioxide fluxes in a minerotrophic fen. *Glob Change Biol* 16:1762–1776
- Stanford JA, Ward JV (2001) Revisiting the serial discontinuity concept. *Regul River* 17:4–5
- Steward AL, von Schiller D, Tockner K et al (2012) When the river runs dry: human and ecological values of dry riverbeds. *Front Ecol Environ* 10:202–209
- Strahler AN (1957) Quantitative analysis of watershed geomorphology. *Civ Eng* 101:1258–1262
- Tamooch F, Borges AV, Meysman FJ, Van Den Meersche K, Dehairs F, Merckx R, Bouillon S (2013) Dynamics of dissolved inorganic carbon and aquatic metabolism in the Tana River Basin, Kenya. *Biogeosciences* 10:6911–6928
- Teodoru CR, Nyoni FC, Borges VA, Darchambeau F, Nyambe I, Bouillon S (2015) Dynamics of greenhouse gases (CO_2 , CH_4 , N_2O) along the Zambezi River and major tributaries, and their importance in the riverine carbon budget. *Biogeosciences* 12:2431–2453
- Thauer RK, Kaster AK, Seedorf H, Buckel W, Hedderich R (2008) Methanogenic archaea: ecologically relevant differences in energy conservation. *Nat Rev Microbiol* 6:579–591
- Threatened Species Scientific Committee (TSSC) (2005) Commonwealth listing advice on temperate highland peat swamps on sandstone. Australian Government Department of Environment. <http://www.environment.gov.au/node/14561>. Accessed on 2 Dec 2015
- Timoner X, Acuña V, von Schiller D, Sabater S (2012) Functional responses of stream biofilms to flow cessation, desiccation and rewetting. *Freshw Biol* 57:1565–1578
- Tweed S, Leblanc M, Bass AM, Harrington GA, Munksgaard NC, Bird MI (2016) Leaky savannas: the significance of lateral carbon fluxes in the seasonal tropics. *Hydrol Process* 30:873–887
- Vachon D, Prairie YT (2013) The ecosystem size and shape dependence of gas transfer velocity versus wind speed relationships in lakes. *Can J Fish Aquat Sci* 70:1757–1764
- von Schiller D, Marcé R, Obrador B, Gómez-Gener L, Casas-Ruiz JP, Acuña V, Koschorreck M (2014) Carbon dioxide emissions from dry watercourses. *Inland Waters* 4:377–382

- von Schiller D, Graeber D, Ribot M, Timoner X, Acunã V, Martí E, Sabater S, Tockner K (2015) Hydrological transitions drive dissolved organic matter quantity and composition in a temporary Mediterranean stream. *Biogeochemistry* 123:429–446
- Wanninkhof R (2014) Relationship between wind speed and gas exchange over the ocean revisited. *Limnol Oceanogr Methods* 12:351–362
- Weiss RF (1974) Carbon dioxide in water and seawater: the solubility of a non-ideal gas. *Mar Chem* 2(3):203–215
- Weyhenmeyer GA, Kortelainen P, Sobek S, Müller R, Rantakari M (2012) Carbon dioxide in boreal surface waters: a comparison of lakes and streams. *Ecosystems* 15:1295–1307
- Weyhenmeyer GA, Kosten S, Wallin MB, Tranvik LJ, Jeppesen E, Roland F (2015) Significant fraction of CO₂ emissions from boreal lakes derived from hydrologic inorganic carbon inputs. *Nat Geosci* 8:933–936
- Xia J, Wu B, Wang G, Wang Y (2010) Estimation of bankfull discharge in the Lower Yellow River using different approaches. *Geomorphology* 117:66–77
- Yamamoto S, Alcauskas JB, Crozier TE (1976) Solubility of methane in distilled water and seawater. *J Chem Eng Data* 21:78–80
- Yvon-Durocher G, Allen AP, Bastviken D et al (2014) Methane fluxes show consistent temperature dependence across microbial to ecosystem scales. *Nature* 507:488–491